

UCRL-JC-130709

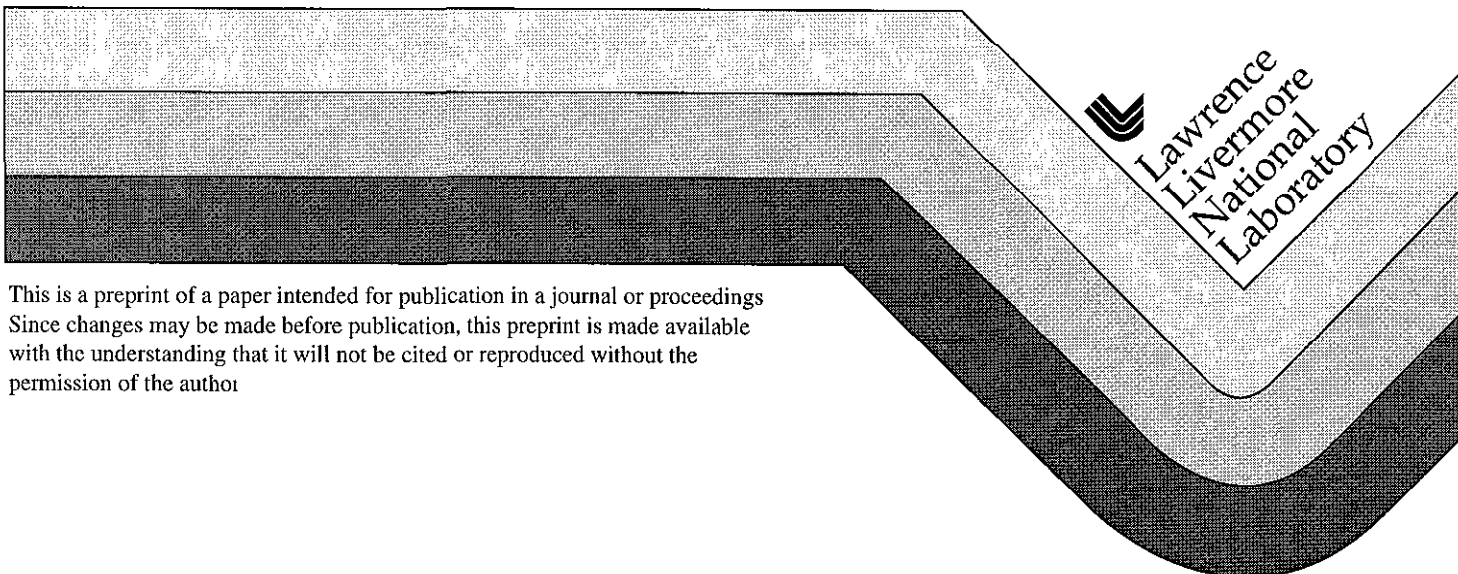
PREPRINT

The Formation of Pre-Sheath Boundary Layers in Electronegative Plasmas

P Vitello

This paper was prepared for submittal to the
Fourth International Workshop on Advanced Plasma Tools & Process Engineering
Millbrae, CA
May 26-27, 1998

May 1998



This is a preprint of a paper intended for publication in a journal or proceedings. Since changes may be made before publication, this preprint is made available with the understanding that it will not be cited or reproduced without the permission of the author.

DISCLAIMER

This document was prepared as an account of work sponsored by an agency of the United States Government. Neither the United States Government nor the University of California nor any of their employees, makes any warranty, express or implied, or assumes any legal liability or responsibility for the accuracy, completeness, or usefulness of any information, apparatus, product, or process disclosed, or represents that its use would not infringe privately owned rights. Reference herein to any specific commercial product, process, or service by trade name, trademark, manufacturer, or otherwise, does not necessarily constitute or imply its endorsement, recommendation, or favoring by the United States Government or the University of California. The views and opinions of authors expressed herein do not necessarily state or reflect those of the United States Government or the University of California, and shall not be used for advertising or product endorsement purposes.

The Formation of Pre-Sheath Boundary Layers in Electronegative Plasmas

P VITELLO

Lawrence Livermore National Laboratory
 7000 East Avenue, L-300
 Livermore, CA 94550
 vitello@llnl.gov

In electronegative plasmas Coulomb scattering between positive and negative ions can lead to the formation of a pre-sheath boundary layer containing the bulk of the negative ions. The negative ion boundary layer forms when momentum transfer from positive to negative ions dominates the negative ion acceleration from the electric field. This condition is met in Inductively Coupled Plasma reactors that operate at low pressure and high plasma density. Simulations of the GEC reactor for Chlorine and Oxygen chemistries using the INDUCT95 2D model are presented showing the pre-sheath boundary layer structure as a function of applied power and neutral pressure.

I. Introduction

The effort by the microelectronics industry to design ultra large scale integrated circuits with ever finer features has spurred the development of high density plasma (HDP) sources [1]. These plasma reactors operate at plasma densities $\gg 10^{10} \text{ cm}^{-3}$ to ensure large ion flux rates to surfaces for rapid etching, low plasma potential (10--30 eV) to minimize surface damage, and low neutral gas pressure (< 30 mTorr) to minimize collisions by ions as they pass from the bulk of the plasma through the sheath. Very high anisotropy of the surface ion flux is essential for generating the sharp walled features with high aspect ratios used in integrated circuits. The so-called Inductively Coupled Plasma (ICP) source is one of the most promising new HDP reactors. One attractive feature of this source is its relative simplicity, e.g., no DC magnetic fields are required for its operation. In addition, control of the plasma density and of the kinetic energy of the ions striking the wafer may be separated in an ICP reactor by use of two driving circuits, one powering the induction coils and a second attached to the electrode on which the wafer is situated [2].

Many commercial plasma reactors use complex halogen (Cl_2 , HBr , BCl_3) or fluorocarbon ($\text{C}_x\text{F}_y\text{H}_z$) based chemistries that tend to generate electronegative plasmas. Plasma discharges containing negative ions may have significantly different features from electropositive discharges. Negative ions are trapped by the plasma sheath and must be destroyed within the

plasma. This tends to enhance their interactions with other species in the plasma. Negative ions can also react strongly with positive ions both chemically and through Coulomb collisions. For the low neutral densities and high positive ion densities typical of ICP discharges, negative ion flow can be tightly coupled to that of positive ions through Coulomb scattering momentum transfer. This can lead to the negative ions moving in the same direction as the positive ions. As the negative ions lack sufficient kinetic energy to cross the sheath their flow from the center of the plasma stagnates, and they become trapped in a pre-sheath boundary layer. Such flow can not be described using an ambipolar description and must be treated using the full momentum equation. The thickness of the pre-sheath boundary layer was found to vary with neutral pressure and inductive power, and showed irregular variations in velocity and density.

Experiments have indicated that electronegative plasma discharges show considerable temporal variations and instability. Unstable behavior is common to most electronegative plasmas, having been observed in Cl_2 , CF_4 , O_2 , and SF_6 . It may show up as variation in the energy coupling from the source to the plasma leading to "mode" jumping [3], oscillations in the plasma potential [4], or ion density modulations [5]. Results shown in this paper indicate that Coulomb scattering may strongly contribute to the observed unstable behavior of electronegative plasmas. Specifically, the expulsion of negative ions measured by Tuszewski [5] is indeed very

similar to density variations described in this paper

In order to investigate the effects of Coulomb coupling we have used the 2D fluid plasma discharge model INDUCT95 [6] to numerical simulation Cl_2 and O_2 discharges in an ICP GEC reference cell. The results described here clearly show that Coulomb scattering can lead to the formation of a pre-sheath boundary layer containing most of the negative ions, and to unstable flow

II. Discharge Model

We describe here briefly the numerical plasma simulation model, INDUCT95, which is based on a fluid dynamic treatment of a non-magnetized plasma. INDUCT95 solves a set of two-dimensional (cylindrically symmetric or Cartesian) time-dependent fluid equations for electrons, ions and neutrals self-consistently with Poisson's equation for the electric potential. In addition, rf inductive heating is calculated from a time-averaged solution of Maxwell's equations

Ion motion is governed by the equations of continuity and momentum conservation, which for ion species i are

$$\frac{\partial n_i}{\partial t} = -\vec{\nabla} \cdot n_i \vec{v}_i + \sum_{j=1}^{N_C} R_{ij} \quad (1)$$

$$\frac{\partial m_i n_i \vec{v}_i}{\partial t} = -\vec{\nabla} \cdot (m_i n_i \vec{v}_i \vec{v}_i) + q_i n_i \vec{E} - \vec{\nabla} \cdot (n_i k T_i) - \sum_{j=1}^{N_S} n_i \mu_{ij} v_{ij} (\vec{v}_i - \vec{v}_j) \quad (2)$$

Here n_i and \vec{v}_i give the ion density and velocity, R_{ij} gives the chemical reaction rates leading to changes in the ion density, v_{ij} is the collision frequency, m_i is the ion mass, q_i is the ion charge, T_i is the ion temperature, μ_{ij} is the reduced mass, and \vec{E} is the electric field. The ion temperature was held fixed for the current simulations. The sums run over the total number of chemical reactions, N_C , and the total number of species, N_S . Chemical interactions treated include ionization, attachment, and recombination. The collision frequency is calculated using

$$v_{ij} = n_j v_{ij}^r \sigma_{ij} \quad (3)$$

where σ_{ij} is the momentum transfer cross-section, and

$$v_{ij}^r = \left[\frac{8kT_i}{\pi m_i} + \frac{8kT_j}{\pi m_j} + (\vec{v}_i - \vec{v}_j) \cdot (\vec{v}_i - \vec{v}_j) \right]^{1/2} \quad (4)$$

is the relative velocity. For scattering between ions and neutrals the cross section was determined from drift velocity data where it was available. Otherwise, hard sphere cross sections based on Lenard-Jones parameters were used. For ion-ion scattering, the shielded Coulomb momentum cross section was used. For negative ions, momentum transfer from ion-ion Coulomb scattering was found to dominate that from ion-neutral scattering in regions of high positive ion flux. We show here that Coulomb scattering can lead to very strong modifications of the discharge structure.

The electron fluid model consisted of the electron continuity and energy balance equations

$$\frac{\partial n_e}{\partial t} = -\vec{\nabla} \cdot \vec{\Gamma}_e + \sum_{j=1}^{N_C} R_{ej} \quad (5)$$

$$\frac{\partial W_e}{\partial t} = -\vec{\nabla} \cdot \vec{Q}_e - e \vec{\Gamma}_e \cdot \vec{E} + P_{ind} - P_{coll} \quad (6)$$

where

$$\vec{\Gamma}_e = - \left[\frac{en_e \vec{E} + \vec{\nabla} \cdot (n_e k T_e)}{m_e v_{eN}} \right] \quad (7)$$

is the electron flux in the drift-diffusion approximation, and

$$\vec{Q}_e = \left(\frac{5}{2} - \frac{d \ln v_{eN}}{d \ln T_e} \right) \left[\vec{\Gamma}_e k T_e - \frac{n_e k T_e}{m_e v_{eN}} \vec{\nabla} \cdot (k T_e) \right] \quad (8)$$

is the electron energy flux. The electron density is given by n_e , $W_e = \frac{3}{2} n_e k T_e$ is the electron thermal energy, m_e is the electron mass, v_{eN} is the total electron-neutral collision frequency (summed over all neutral species), P_{ind} is the time-averaged power per unit volume absorbed by the electrons due to the inductive rf fields, and P_{coll} is the energy loss per unit volume due to electron-neutral collisions.

Neutral flow and chemistry are treated in INDUCT95 assuming constant total pressure and a uniform neutral temperature. For the results presented here a value of 600 °K was used for the neutral temperature. The separate neutral species number densities were calculated from their

continuity equation including binary diffusion and source terms

$$\frac{\partial n_n}{\partial t} = -D_n \nabla^2 n_n + \sum_{j=1}^{N_c} R_{nj} \quad (9)$$

Detailed surface chemistry reaction for de-citation of meta-stables, neutralization of ions, and recombination of neutral species were included on all surfaces

Space-charge electric fields were determined self-consistently using Poisson's equation

$$\vec{\nabla} \cdot \epsilon \vec{\nabla} \phi^{n+1} = -\left(\sum_{i=1}^{N_i} q_i n_i^{n+1} - n_e^{n+1}\right) \quad (10)$$

where ϵ is the local dielectric constant and N_i gives the number of ion species. To avoid disastrous amplification of the electrostatic field when time steps larger than the Dielectric Relaxation time scale were used we solve Poisson's equation at the future time level using time advanced charge densities. As ionization and chemical reactions do not affect the space charge density, only terms due to flow need be considered when approximating the time advanced densities. For the electron density equations (5) and (7) were used to determine

$$\begin{aligned} n_e^{n+1} &= n_e^n + \delta t \left(\frac{\partial n_e}{\partial t} \right)^n \\ &= n_e^n - \delta t \vec{\nabla} \cdot \left[\frac{en_e^n \vec{\nabla} \phi^{n+1}}{m_e V_{eN}^n} - \frac{\vec{\nabla}(n_e^n kT_e^n)}{m_e V_{eN}^n} \right] \quad (11) \end{aligned}$$

Here the superscript n implies the current time level variables, and superscript n+1 signifies the future time level variables to be solved for. Upon replacing n_e^{n+1} in equation (10) from equation (11), terms involving ϕ^{n+1} were combined with ϵ being replaced by an effective dielectric tensor. Due to their slower response to the electric field, the time advanced ion densities were calculated using an explicit extrapolate from previous time level data.

The geometry used for the GEC reference cell was similar to that described in our previous paper [6]. The gas feed for the current study was moved to the side to simulate inflow from an access port, and the interior of the lower electrode was modeled as a dielectric which extended to the lower boundary [3]. Boundary conditions for the potential along the cylinder that contained the numerical simulations were

$\phi = 0$ at metal surfaces and $\vec{n} \cdot \vec{\nabla} \phi = 0$ at openings and dielectric surfaces, where \vec{n} is the normal vector to the surface. For electrons, the plasma boundary condition on the outward flux onto metal and dielectric surfaces was set to $0.25 n_e c_s e^{-e\delta\phi/kT_e} \vec{n}$, where n_e is the electron density at the computational mesh point adjacent to the surface, c_s is the mean electron velocity at that point, and $\delta\phi$ is the potential drop from the computational mesh point to the surface. An inward electron flux due to secondary emission was added to the outward flux to determine the net flux. The value used for the secondary electron emission coefficient was kept small ($\gamma_s = 0.01$), and was used for stability purposes only. At openings to the chamber the electron flux was set equal to the total outward ion flux. For the electron energy flux, a boundary value of $2kT_e \vec{\Gamma}_e$ was used onto metal and dielectric surfaces. At openings the normal component of the electron temperature gradient was set to zero. Upwind differencing was used for ions at all surfaces. If the outward component of velocity was positive, then ions were simply allowed to escape. If the outward component was negative, then the velocity at the surface was set to zero. Note that INDUCT95 treats the sheath as part of the solution domain and does not make use of a sheath model.

III. Results

We show model simulation results here for chlorine and oxygen discharges. The chlorine atomic data set used was described in Bukowski [6]. The oxygen atomic data set was similar to that described in Lieberman and Lichtenberg [7], and will be characterized in detail in a following study. The inflow rate used in our modeling was 30 sccm. Simulation results were found to be weakly dependent upon the inflow rate or the values used for wall recombination. While INDUCT95 is capable of treating biasing both from inductive coil capacitive coupling and from the lower electrode, these effects were neglected for the current study.

A study was made of discharges of pure chlorine and pure oxygen over a wide range of pressures and inductive powers. Results are presented here for chlorine at 25mTorr and 200W, 25mTorr and 50W, and 10mTorr and 200W. These

parameters show the typical behavior of the discharge for several different regimes. For comparison, and oxygen discharge at 10 mTorr and 200 W is shown.

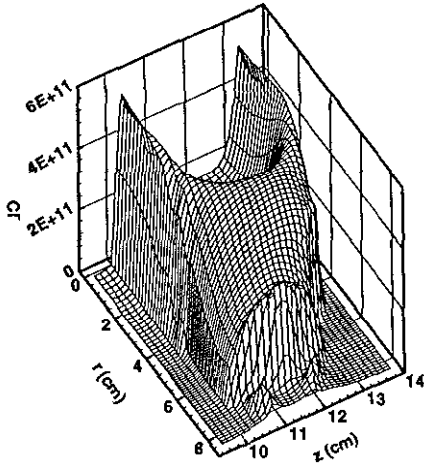


Figure 1 Cl⁻ density at the cavity center for 25mTorr and 200W

Coulomb scattering was found to profoundly modify the density profiles for all cases of chlorine shown here. Figures 1–3 show the Cl⁻ densities in the region between the electrodes for the three cases. The corresponding flow fields for the Cl⁻ flux are shown in Figures 4–6. For 25mTorr and 200W the Cl⁻ ions form a thick boundary layer in the pre-sheath. At lower pressure and fixed power (see Figures 2 and 5), the negative ions were more strongly expelled from the bulk of the discharge and the boundary layer became thinner and highly irregular. The Cl⁻ flow field shows noticeable turbulence at the lower pressure. Dropping the power at fixed

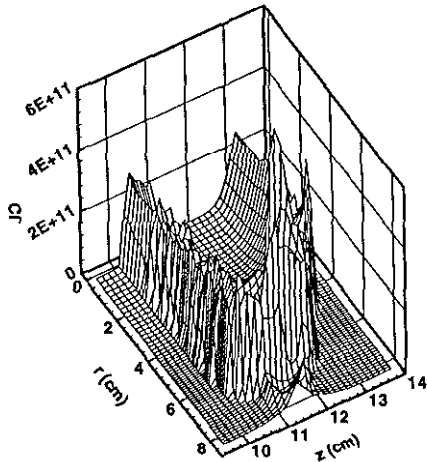


Figure 2 Cl⁻ density at the cavity center for 10mTorr and 200W

pressure leads to a flat topped density profile for Cl⁻. This was the result of the boundary layer broadening until it filled the volume of the discharge (see Figures 3 and 6).

For all chlorine discharges shown, negative ions experienced larger ion-ion momentum transfer than from ion-neutral scattering. Positive ions were found to generally have the opposite behavior, with ion-neutral scattering causing significantly larger momentum transfer than scattering with negative ions. Only for the 25mTorr and 50W case was Coulomb momentum transfer found, for positive ions, to be of the same order as that from neutral scattering.

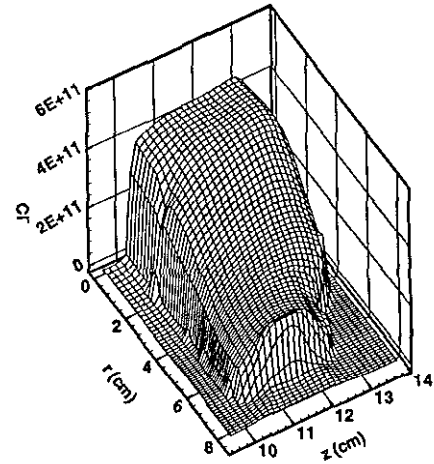


Figure 3 Cl⁻ density at the cavity center for 25mTorr and 50W

In the regime where Coulomb scattering dominates ion-neutral scattering, and where the ion pressure and advection terms are negligible, equation (2) can be used to approximate the Cl⁻ ion velocity as

$$\bar{v}_{\alpha^-} \approx \frac{\left(-\frac{e\bar{E}}{m_{\alpha^-}} + \frac{1}{2}v_{\alpha^-\alpha^+}\bar{v}_{\alpha^+} + \frac{2}{3}v_{\alpha^-\alpha_i^+}\bar{v}_{\alpha_i^+} \right)}{\left(\frac{1}{2}v_{\alpha^-\alpha^+} + \frac{2}{3}v_{\alpha^-\alpha_i^+} \right)} \quad (12)$$

For significantly large Coulomb collision frequencies and positive ion velocities, the net Cl⁻ velocity will have the same sign as the positive ions. This is clearly seen in Figures 4–5 in the center of the discharge. As the negative ions lack sufficient kinetic energy to cross the sheath and leave the plasma, any negative ion flow from the plasma center will be stopped

before reaching the sheath, with the trapped negative ions forming a boundary layer

The structure of the negative ion density profile is strongly dependent upon both the pressure and inductive power. For 25mTorr and 200W, the center of the discharge was only mildly electronegative, and the Coulomb momentum transfer from positive ions to negative ions resulted in merely a slight decrease in the positive ion outflow velocity. Decreasing the pressure from 25mTorr to 10mTorr had several effects. The degree of Cl_2 disassociation to Cl increased, leading to a strong reduction in the creation rate of negative ions. The resulting lower Cl^- density reduced the Coulomb drag on positive ions, which also underwent less scattering with neutrals at the lower pressure. This increase in the positive ion velocity resulted in the negative ions being more readily pushed out and a thinner boundary layer was generated.

At lower pressure, knots of enhanced Cl^- density appeared in the boundary layer. These knots form where negative ions being push outward from the center of the plasma ran into inward moving negative ions. The inward moving Cl^- ions came from regions of low positive ion density where Coulomb scattering with positive ions was insignificant. Turbulent behavior was observed to be especially prevalent near the ends on the electrodes where strong inflow of negative ions occurred.

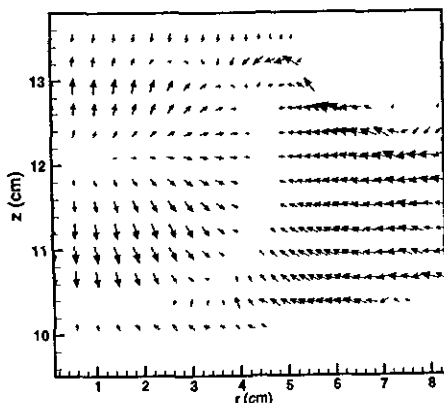


Figure 4 Cl^- flux ($\text{cm}^{-2}\text{s}^{-1}$) at the cavity center for 25mTorr and 200W

As opposed to dropping the neutral pressure, the effect of decreasing the inductive power was to broaden the boundary layer (see Figure 3). This was not due to a lessening of Coulomb scattering

for negative ions, but was instead due to an increase in the Coulomb drag on positive ions. At lower inductive power, the degree of Cl_2 disassociation decreased. At the higher Cl_2 density, negative ions were more rapidly produced and the degree of electronegativity increased. The larger negative ion density increased the momentum lost by positive ions through Coulomb scattering. This resulted in a significant decrease in positive ion velocities in the pre-sheath. In this region, negative ions still experienced a significant outward push from Coulomb with positive ions. With the reduced positive ion velocity, the Coulomb momentum transfer was however less than that from the electric field (see Figure 6).

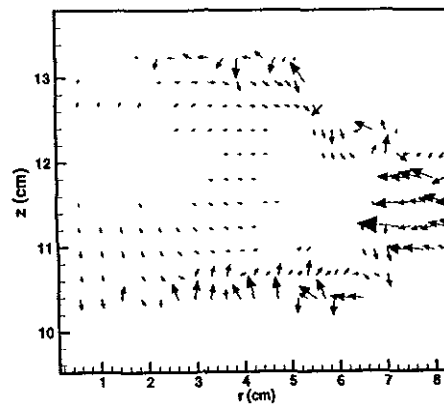


Figure 5 Cl^- flux ($\text{cm}^{-2}\text{s}^{-1}$) at the cavity center for 10mTorr and 200W

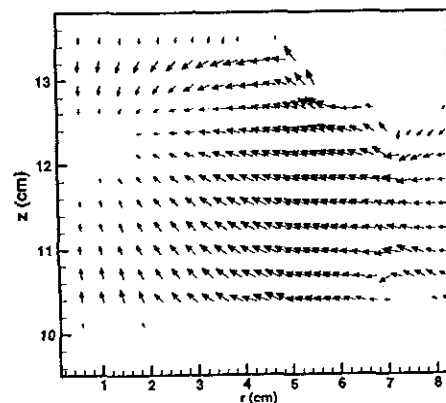


Figure 6 Cl^- flux ($\text{cm}^{-2}\text{s}^{-1}$) at the cavity center for 25mTorr and 50W

We consider next how dependent our results are upon the chemistry of the discharge gas. Figures 7—8 show the O^- density and flux flow field for an oxygen discharge at 10mTorr and 200W.

The oxygen plasma density was markedly less than that calculated for chlorine. Both positive and negative ion densities were roughly a factor of 10 smaller. The oxygen plasma also was less confined than the chlorine plasma. Electron and ion densities were appreciable well beyond the electrodes. In fact, the bulk of the production of O^- was observed to take place at large radii. Inflow of these ions is seen in Figure 8. While Coulomb scattering with positive ions contributed significantly to the negative ion momentum balance, the positive ion density was too small to slow the incoming O^- ions, which were pulled inward by the electric field. Details of ICP discharges are clearly dependent upon the plasma chemistry.

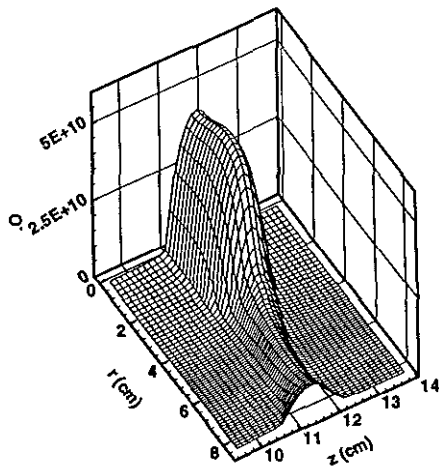


Figure 7 O^- density at the cavity center for 10mTorr and 200W

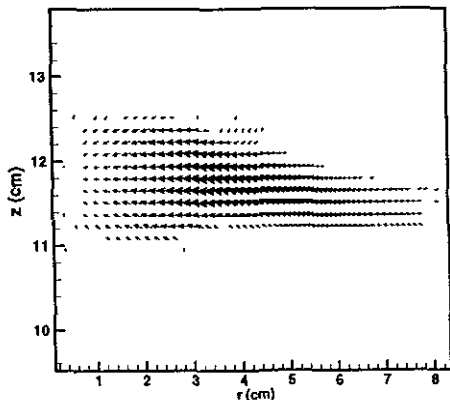


Figure 8 O^- flux ($cm^{-2}s^{-1}$) at the cavity center for 10mTorr and 200W

IV. Conclusions

For low neutral densities and high positive ion densities, negative ion flow can be tightly

coupled to that of positive ions through Coulomb scattering momentum transfer. Negative ions may experience larger momentum transfer from positive ions than from neutrals. This can lead to the formation of a narrow, unstable, pre-sheath boundary layer. The structure of the boundary layer was found to vary with neutral pressure and inductive power. Plasma conditions were found to depend on the discharge chemistry to the extent that for equal neutral pressure and power, extremely different negative ion structure was observed for chlorine and oxygen. Further studies of Coulomb scattering in ICP reactor systems should be undertaken with a more detailed treatment of the ion flow. To correctly study how Coulomb scattering may lead to unstable behavior, temperature dependent ion-neutral reaction rates should be used.

Acknowledgments

This work was performed under the auspices of the U S Department of Energy at the Lawrence Livermore National Laboratory under contract W-7405-ENG-48

References

- [1] J Hopwood, *Plasma Sources Sci Technol*, **7**, 109 (1992)
- [2] R Patrick, P Schoenborn, H Toda, and F Bosc, *J Vac Sci Technol A*, **11**, 1296 (1993)
- [3] P A Miller, G A Hebner, K E Greenberg, P D Pochan, and B P Aragon, *J Res Natl Int Stand Technol*, **100**, 427 (1995)
- [4] M Nasser, Y Ohtsu, G Tochtani and H Fujita, *Jpn J Appl Phys*, **36**, 4722 (1997)
- [5] M Tuszewski, *J Appl Phys*, **79**, 8967 (1996)
- [6] J D Bukowski, D B Graves, P Vitello, *J App Phys*, **80**, 2614 (1996)
- [7] M A Lieberman and A J Lichtenberg, "Principles of Plasma Discharges and Materials Processing," Wiley-Interscience, New York (1994)

Technical Information Department • Lawrence Livermore National Laboratory
University of California • Livermore, California 94551

